Improving the normalized difference built-up index to map urban built-up areas using a semiautomatic segmentation approach

Chunyang He[ab]; Peijun Shi[a]; Dingyong Xie[b]; Yuanyuan Zhao[ab]

[a] State Key Laboratory of Earth Surface Processes and Resource Ecology, Beijing Normal University, Beijing, China [b] College of Resources Science and Technology, Beijing Normal University, Beijing, China

First published on: 26 April 2010

PLEASE SCROLL DOWN FOR ARTICLE

Taylor & Francis
Taylor & Francis Group

Improving the normalized difference built-up index to map urban built-up areas using a semiautomatic segmentation approach

CHUNYANG HE*†‡, PEIJUN SHI†, DINGYONG XIE‡ and
YUANYUAN ZHAO†‡

†State Key Laboratory of Earth Surface Processes and Resource Ecology, Beijing Normal
University, Beijing 100875, China
‡College of Resources Science and Technology, Beijing Normal University, Beijing
100875, China

Remote sensing images are useful for monitoring the spatial distribution and growth of urban built-up areas because they can provide timely and synoptic views of urban land cover. Although the normalized difference built-up index (NDBI) is useful to map urban built-up areas, it still has some limitations. This study sought to improve the NDBI by using a semiautomatic segmentation approach. The proposed approach had more than 20% higher overall accuracy than the original method when both were implemented simultaneously at the National Olympic Park (NOP), Beijing, China. One reason for the improvement is that the proposed NDBI approach separates urban areas from barren and bare land to some extent. More importantly, the proposed method eliminates the original assumption that a positive NDBI value should indicate built-up areas and a positive normalized difference vegetation index (NDVI) value should indicate vegetation. The new method has improved universality and lower commission error compared with the original method.

1. Introduction

Urban land accounts for a small fraction of the Earth's surface area but has a disproportionate influence on its surroundings in terms of mass, energy and resource fluxes (Lambin and Geist 2001). Mapping urban land in a timely and accurate manner is indispensible for watershed run-off prediction and other planning applications (Small 2003). Remote sensing images are useful for monitoring the spatial distribution and growth of urban built-up areas because of their ability to provide timely and synoptic views of land cover (Guindon *et al.* 2004, Xu 2008, Bhatta 2009, Griffiths *et al.* 2010). Over the past two decades, researchers have become increasingly interested in using remotely sensed imagery to address urban and suburban problems (Jacquin *et al.* 2008). A number of techniques for automatically mapping urban land cover using satellite imagery have been formulated, applied and evaluated. These techniques can be broadly grouped into two general types: (1) those based on the classification of the input data, including pixel- and object-based classifications (Guindon *et al.* 2004, Cleve *et al.* 2008) and (2) those based on directly segmenting the indices, such as the commonly used normalized difference vegetation index (NDVI) (Zha *et al.* 2003, Zhang *et al.* 2005). However, the spatial and spectral

---

*Corresponding author. Email: hcy@bnu.edu.cn

variabilities of urban environments present fundamental challenges to deriving accurate remote sensing-based products for urban areas (Powell *et al.* 2007). Efforts to improve automatic mapping of urban land use using satellite imagery are thus still worthwhile.

Zha *et al.* (2003) proposed the normalized difference built-up index (NDBI) to automatically map urban built-up areas. The method takes advantage of the unique spectral responses of built-up areas and other land covers. Built-up areas are effectively mapped through the arithmetic manipulation of recoded NDVI and NDBI images derived from Landsat Thematic Mapper (TM) imagery. However, the approach proposed by Zha *et al.* (2003) recodes the derived NDBI and NDVI images to create binary images under the assumption that a positive value of NDBI should indicate built-up areas and a positive value of NDVI should indicate vegetation. As discussed by Zha *et al.* (2003), with this recoding process, their approach is unable to separate urban areas from barren and bare land. They suggested that the universality of the approach needed to be tested in other geographic areas because of the actual complicated spectral response patterns of vegetation.

In the light of the original NDBI approach's advantages and drawbacks, this study tried to improve it using a semiautomatic segmentation approach. The proposed NDBI approach and the original NDBI approach were also simultaneously applied to the National Olympic Park (NOP), Beijing, and the results were evaluated and compared with those of Zha *et al.* (2003).

2. Method

2.1 *Original NDBI approach*

Based on the analysis of the unique spectral responses of built-up areas and other land covers in seven Landsat TM bands, the original NDBI approach developed by Zha *et al.* (2003) was implemented as three arithmetic manipulations of TM bands 3–5, followed by recoding. First, a continuous NDVI image $NDVI_c$ was obtained by the following equation:

$$NDVI_c = \frac{band4 - band3}{band4 + band3} \tag{1}$$

To facilitate the subsequent process, the derived $NDVI_c$ was recoded to create a binary NDVI image $NDVI_b$ with 245 for all pixels having positive indices (vegetation) and 0 for all remaining pixels of negative indices.

Second, the continuous NDBI image $NDBI_c$ was produced by the following equation:

$$NDBI_c = \frac{band5 - band4}{band5 + band4} \tag{2}$$

The derived $NDBI_c$ was then recoded to create a binary NDBI image $NDBI_b$ with 0 for those pixels having a negative value or 254 for those having a positive value.

Third, the built-up areas were extracted by the following equation:

$$BU_b = NDBI_b - NDVI_b \tag{3}$$

where BU_b is the resultant binary image with only the built-up and barren pixels having positive value, thus allowing built-up areas to be mapped automatically (Zha *et al.* 2003).

2.2 *Proposed NDBI approach*

The proposed NDBI approach was implemented as follows: first, the continuous NDVI image $NDVI_c$ and the continuous NDBI image $NDBI_c$ were directly derived from the Landsat TM image following equations (1) and (2), respectively.

Second, the continuous image BU_c was produced by the following equation:

$$BU_c = NDBI_c - NDVI_c \qquad (4)$$

Unlike the binary image BU_d obtained with the original NDBI approach, BU_c is one continuous image. The greater the value of a pixel in BU_c is, the higher is the possibility of the pixel being a built-up area.

Third, using one optimal threshold value, the continuous image BU_c was segmented into one binary image with the built-up area being 1 and other areas being 0. Often, the optimal threshold value to segment one continuous image is determined according to the empirical strategies or from manual trial-and-error procedures. These procedures usually require a more experienced image analyst and a long trial time (Chen *et al.* 2003). Chen *et al.* (2003) presented the double-window flexible pace search (DFPS) approach to determine the optimal threshold value between change and non-change pixels when detecting land use/cover change. This semiautomatic method only requires the involvement of an image analyst during the selection of typical training samples and thus has an advantage of effectively determining the optimal threshold value to segment one continuous image to detect land use/cover change (Chen *et al.* 2003). Using the idea of the DFPS, we developed a semiautomatic approach to determine the optimal threshold value to segment BU_c to extract built-up areas. The basic idea of the semiautomatic approach is to select a threshold value from the training samples, assuming that the threshold value leading to the maximum accuracy in extracting the built-up area within the training samples is also optimal for the entire BU_c. The process mainly involves the following four steps.

First, some typical built-up areas are chosen as the sample areas by visual interpretation of the image. The criteria for selecting sample areas are (1) training samples should include only built-up pixels and (2) training samples should be 'islands' encircled by non-built-up pixels.

Second, the search range and pace are determined according to the analysis of the histogram of BU_c. The search range can be set as a difference between the minimum value a and the maximum value b of BU_c. The first search pace (increment) P_1 may be calculated according to the following formula:

$$P_1 = \frac{b-a}{m} \qquad (5)$$

where m is a positive integer that determines the number of potential thresholds in a search process and can be set manually. The potential thresholds to detect built-up pixels from the training samples in the search process are given within the range of (a, b) as $b - P_1$, $b - 2P_1$, ... It should be noted that the size of the manually set m does not affect the search efficiency and the final results. A large m increases the number of potential thresholds during one search, but it decreases the number of searches.

Third, the success rate of built-up-area extraction is defined to evaluate the performance of each potential threshold value during one search process for identifying built-up/non-built-up pixels. The success rate L_k is calculated for a potential threshold value of k as

$$L_k = \frac{(A_{k1} - A_{k2})}{A} \times 100\% \qquad (6)$$

where A_{k1} is the number of built-up pixels detected inside all training patches, A_{k2} is the number of built-up pixels that are detected incorrectly and A is the total number of pixels within all training patches. After all the L_k for all the m thresholds in one search are obtained, the maximum and minimum values of L_k can be found and designated as L_{max} and L_{min} during this search process. If the two parameters do not satisfy the exit conditions described in the fourth step, a new search begins. The new search range is set in the range $(k_{max} - P_1, k_{max} + P_1)$, and a new smaller search pace is set based on the modified search range with equation (5). Here, k_{max} is the potential threshold value corresponding to L_{max} in the search process.

Finally, the second and third steps involve an iterative process, which will be terminated when the following equation is satisfied:

$$L_{max} - L_{min} \leq \delta \qquad (7)$$

where L_{max} and L_{min} are the maximum and minimum values of the success rate in one search process, and δ is an acceptable error constant. The threshold value corresponding to L_{max} is considered to be an optimal threshold value to extract the built-up areas from BU_c when the change of search pace has little influence on the result of built-up area extraction.

3. Case study: mapping built-up areas in the National Olympic Park (NOP), Beijing

3.1 *Study area and data*

The NOP, located in northern Beijing, was selected as the study area to evaluate the performance of the proposed approach (figure 1). The NOP covers 12.15 km^2. Massive construction began at the NOP in 2000 in preparation for the 2008 Olympic Games in Beijing. A Level 1R Landsat Enhanced Thematic Mapper (ETM+) image acquired on 19 May 2001 was used as the test image for radiometric correction. This image had high quality and fully covered the study area. Some auxiliary data were collected, including a 1:50,000-scale topographic map for 1972 and a 1:100,000-scale land use map for 2000. In addition, one IKONOS image acquired on 26 April 2001 was also used to assist the accuracy assessment because of its fine resolution compared with the Landsat ETM+ image.

3.2 *Image preprocessing*

High-precision geometric registration is the basic requirement of image preprocessing (Guindon *et al.* 2004). First, the Landsat ETM+ image was geometrically corrected according to the Universal Transverse Mercator projection at 30×30-m resolution, using second-order polynomial and bilinear interpolation. Forty ground control points were collected from the 1:50,000 topographic map. The root mean square error was less than 1 pixel. Then, the boundary of the NOP, digitized into a GIS database, was used to clip the study area from images (figure 2).

3.3 *Mapping built-up area*

Following equations (1), (2) and (4), the continuous NDVI image NDVI$_c$, the continuous NDBI image NDBI$_c$ and the continuous image BU$_c$ were directly derived
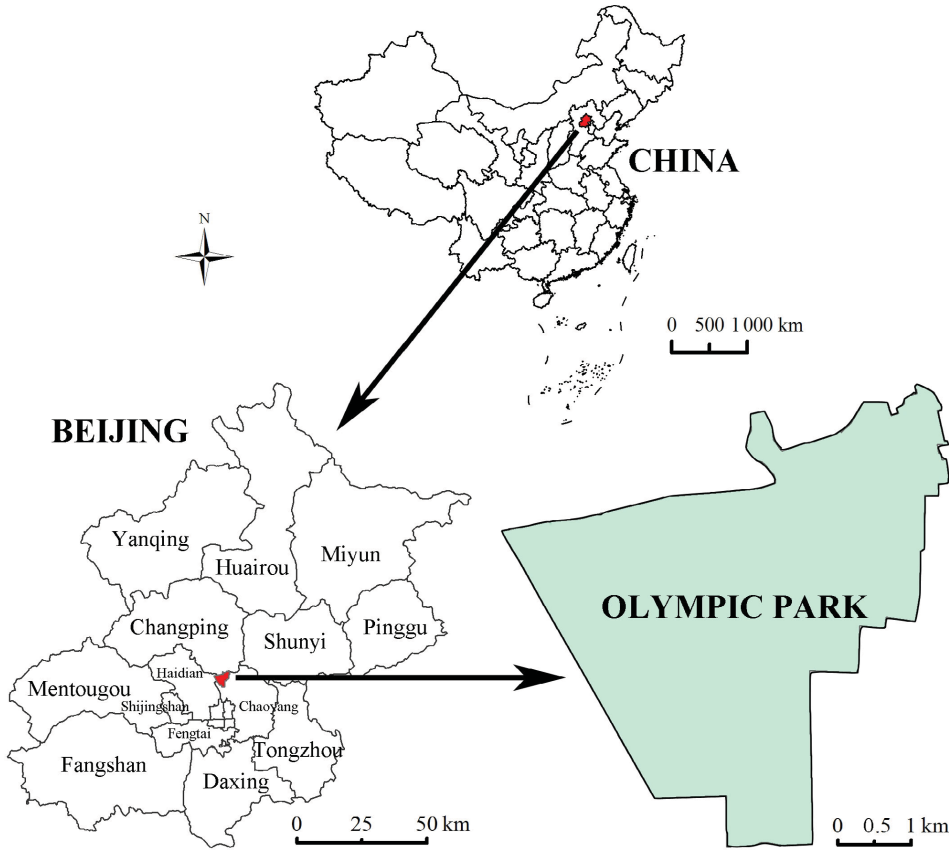
Figure 1.   The study area.

from the Landsat ETM+ image. To assist the process of determining the optimal threshold value, $NDVI_c$, $NDBI_c$ and BU_c were first normalized into (0, 255) with the following equation (figure 3):

$$N = \frac{(T - T_{\min})}{(T_{\max} - T_{\min})} \times 255 \tag{8}$$

where N is the pixel value of the normalized image, T is the pixel value of the inputted image and $T_{\max}$ and $T_{\min}$ represent the maximum and minimum pixel values of the inputted image, respectively.

From the analysis of the histogram of BU_c, the search range was set (0, 226) with the initial pace of 20. The semiautomatic segmentation approach was then used to determine the optimal threshold value as 102; pixels with values over 102 were extracted from BU_c as built-up areas (figure 4(c)).

3.4   *Accuracy assessment*

To evaluate the performance of the proposed NDBI method, a stratified random sampling method was used for accuracy assessment with 80 samples each of built-up areas and of non-built-up areas (Congalton 1991). The results showed that the total
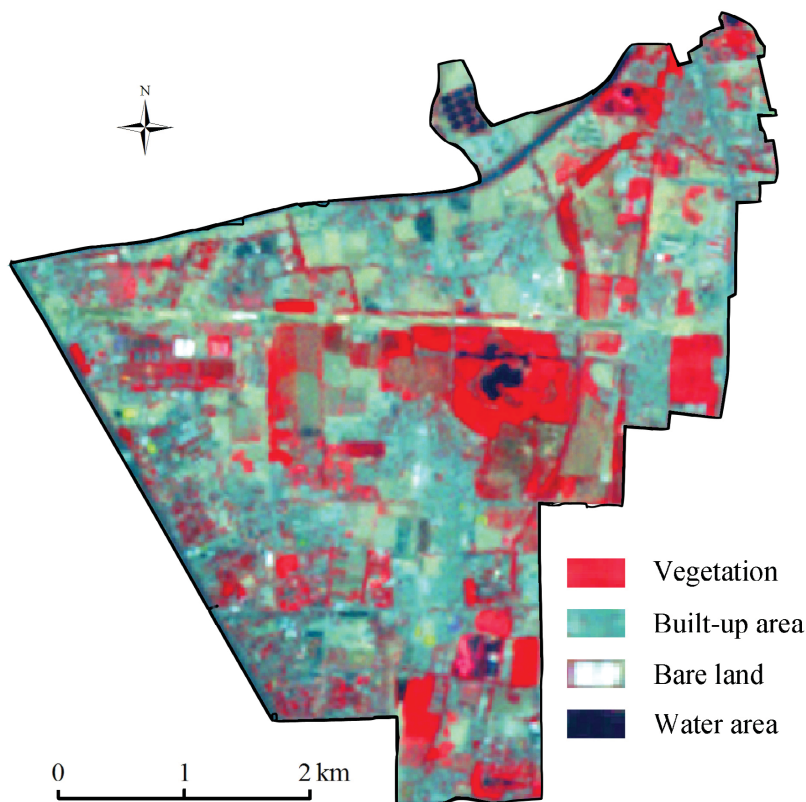
Figure 2. The used Landsat ETM+ image of the study area. Note: The image is a standard false colour composite: band 4, red; band 3, green; and band 2, blue.

accuracy of the proposed NDBI approach was 86.30% (table 1). In addition, the original NDBI approach was also used to produce binary built-up-area imagery (figure 4(*b*)), and the same accuracy assessment was implemented to compare the accuracies of the two approaches. The results showed that the overall accuracy of the original NDBI approach was 64.38%. The proposed approach improved the overall accuracy by over 20%. Interpretation of the original imagery (figure 4(*a*)) and the resultant images (figure 4(*b*) and (*c*)) showed that the original approach had obvious commission error, showing some vegetation as built-up area (see the area in the yellow rectangle in figures 4(*a*)–(*c*)). The proposed approach separated urban areas from barren and bare land to some extent and reduced the commission error of the original approach.

4.   Conclusion and discussion

The original NDBI approach is an effective method for automatically mapping urban built-up areas using the Landsat TM imagery, offering easy operation and independence of sample selection by manual operation. However, this approach also has some limitations associated with recoding the derived NDBI imagery and NDVI imagery to create a binary image and assuming that positive NDBI value should indicate built-up areas and positive NDVI value should indicate vegetation. Because
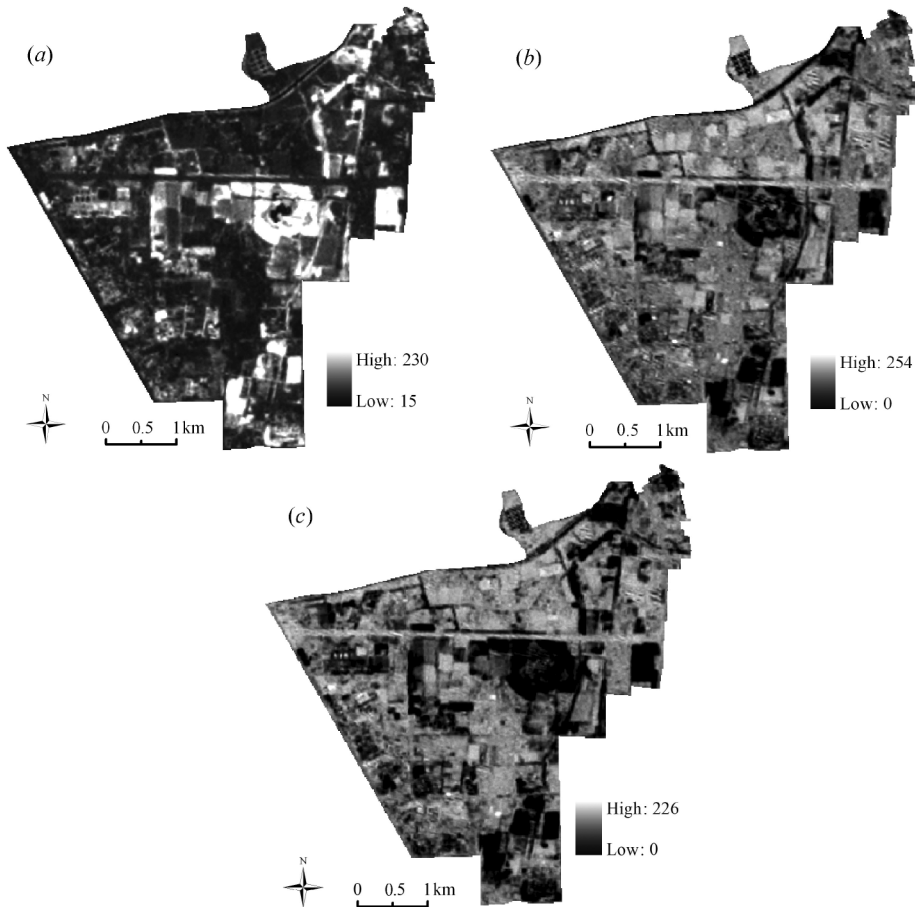
Figure 3. The obtained continuous NDVI, NDBI and built-up-area images of the study area. Note: (*a*) is the continuous NDVI image, (*b*) is the continuous NDBI image and (*c*) is the continuous built-up area image.

of this recoding process, the original approach was unable to separate urban areas from barren and bare land. In this study, the original approach also suffered from commission error, showing some vegetation as built-up area because of the complicated spectral response patterns of vegetation.

In this letter, the original NDBI approach was improved by directly segmenting the resultant continuous image with an optimal threshold value determined by a semiautomatic segmentation approach based on the idea of the DFPS. In this case study, our proposed approach had over 20% higher overall accuracy than the original approach when implemented simultaneously for the NOP, Beijing. One reason for the improvement is that the proposed approach separated urban areas from barren and bare land to some extent. More importantly, however, the proposed approach abolishes the assumption that a positive NDBI value should indicate a built-up area whereas a positive NDVI value should indicate vegetation. The proposed approach improves the universality and reduces the commission error of the original NDBI approach.
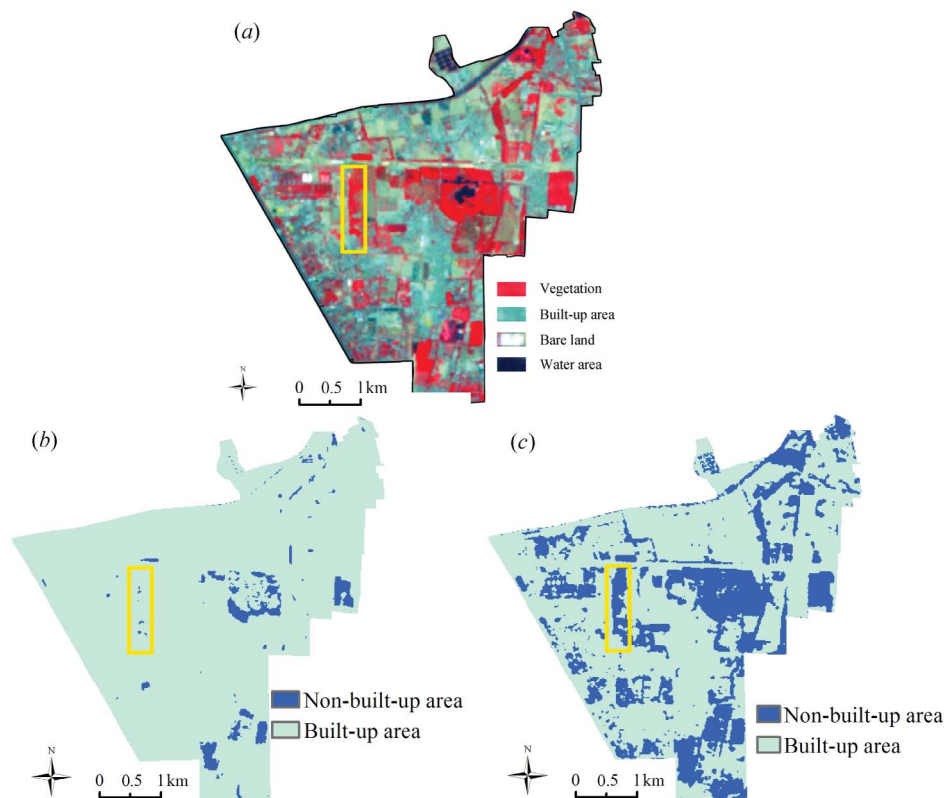
Figure 4. Comparison of the results by the original and proposed approaches. Note: (*a*) is the Landsat ETM+ image used in this study, (*b*) is the resultant binary image of the built-up and non-built-up areas by the original approach and (*c*) is the resultant binary image of the built-up and non-built-up areas by the proposed approach; the area in the yellow rectangle in each panel is where the original approach produced obvious commission error, giving vegetation as a built-up area.

Table 1. Accuracy assessment of the resultant images.

	Overall accuracy (%)	Omission error (%)	Commission error (%)	κ coefficient
NDBI approach	64.38	3.45	47.17	0.35
Improved NDBI approach	86.30	0	18.87	0.70

However, like the original NDBI approach, the proposed approach also has some limitations because it is a semiautomatic approach depending on training sample selection by manual operation. It, therefore, relies to some degree on the experience and skill of the image analyst. In addition, the proposed approach cannot entirely separate bare land and built-up areas because of their similar spectral character in Landsat ETM+ imagery. Users should consider the trade-offs between efficiency and accuracy when choosing between the original and proposed NDBI approaches.

References

BHATTA, B., 2009, Analysis of urban growth pattern using remote sensing and GIS: a case study of Kolkata, India. *International Journal of Remote Sensing*, **30**, pp. 4733–4746.

CHEN, J., GONG, P., HE, C., PU, R. and SHI, P., 2003, Land use/cover change detection using improved change vector analysis. *Photogrammetric Engineering and Remote Sensing*, **69**, pp. 369–379.

CLEVE, C., KELLY, M., KEARNS, F. and MORITZ, M., 2008, Classification of the wildland–urban interface: a comparison of pixel- and object-based classifications using high-resolution aerial photography. *Computers, Environment and Urban Systems*, **32**, pp. 317–326.

CONGALTON, R., 1991, A review of assessing the accuracy of classifications of remotely sensed data. *Remote Sensing of Environment*, **37**, pp. 35–46.

GRIFFITHS, P., HOSTERT, P., GRUEBNER, O. and VAN DER LINDEN, S., 2010, Mapping megacity growth with multi-sensor data. *Remote Sensing of Environment*, **114**, pp. 426–439.

GUINDON, B., ZHANG, Y. and DILLABAUGH, C., 2004, Landsat urban mapping based on a combined spectral–spatial methodology. *Remote Sensing of Environment*, **92**, pp. 218–232.

JACQUIN, A., MISAOVA, L. and GAY, M., 2008, A hybrid object-based classification approach for mapping urban sprawl in periurban environment. *Landscape and Urban Planning*, **84**, pp. 152–165.

LAMBIN, E.F. and GEIST, H., 2001, Global land use and land cover change: what have we learned so far? *Global Change News Letter*, **46**, pp. 27–30.

POWELL, R., ROBERTS, D., DENNISON, P. and HESS, L., 2007, Sub-pixel mapping of urban land cover using multiple endmember spectral mixture analysis: Manaus, Brazil. *Remote Sensing of Environment*, **106**, pp. 253–267.

SMALL, C., 2003, High spatial resolution spectral mixture analysis of urban reflectance. *Remote Sensing of Environment*, **88**, pp. 170–186.

XU, H., 2008, A new index for delineating built-up land features in satellite imagery. *International Journal of Remote Sensing*, **29**, pp. 4269–4276.

ZHA, Y., GAO, Y. and NI, S., 2003, Use of normalized difference built-up index in automatically mapping urban areas from TM imagery. *International Journal of Remote Sensing*, **24**, pp. 583–594.

ZHANG, Q., PAVLIC, G., CHEN, W., FRASER, R., LEBLANC, S. and CIHLAR, J., 2005, A semi-automatic segmentation procedure for feature extraction in remotely sensed imagery. *Computers and Geosciences*, **31**, pp. 289–296.